Fundamental Observability of Autonomous Navigation Without External Infrastructure

Sanjay S, *Researcher, Kepler Nav*

***Abstract*—Autonomous navigation for aerospace and deep-space vehicles operating in infrastructure-denied environments represents a fundamental challenge in estimation theory and nonlinear control [1]–[3]. Conventional approaches, such as X-ray pulsar navigation (XNAV) [4], [5] or signals-of-opportunity (SOOP) [6], [7], frequently treat sensing modalities as isolated hardware implementations, obscuring the mathematical limits of state recovery. In this paper, we establish a sensor-agnostic, infrastructure-independent theoretical framework for 6-dimensional state observability. Beginning from first principles of differential geometry on Lie groups SE(3) [3], [13], we introduce the foundational axiom that navigation is the reconstruction of a vehicle's state trajectory from the time evolution of observables governed by natural system dynamics [14]. Using Lie derivative operator expansions and the Hermann-Krener local weak observability criteria [1], we prove that static single or multi-channel line-of-sight projection observables are rank-deficient (rank $\leq 3 < 6$), rendering instantaneous 6D state recovery impossible. We then prove that continuous trajectory evolution under central gravitational fields restores full-rank observability (rank $= 6$) via the higher-order Lie algebra of the gravity gradient tensor $\mathbf{G}(\mathbf{r})$, provided non-planar trajectory conditions hold. Furthermore, we establish the Doppler-Spatial Duality theorem, formulate the Low-Altitude Geomagnetic Tensor State Determinism conjecture, and validate our analytical proofs through numerical LEO orbit simulations.**

***Index Terms*—Autonomous Navigation, Lie Derivatives, Non-Linear Observability, Hermann-Krener Theorem, Gravity Gradient Tensor, Signals of Opportunity, Position Navigation and Timing (PNT).**

I. Introduction

POSITION, Navigation, and Timing (PNT) systems form the critical backbone of aerospace vehicles, planetary landers, autonomous drones, and defense platforms [4], [8], [10]. For decades, operational guidance has relied heavily on Global Navigation Satellite Systems (GNSS), such as GPS, GLONASS, Galileo, and BeiDou, alongside radiometric tracking via NASA's Deep Space Network (DSN) [11], [12]. However, total dependency on external beacon infrastructure exposes platforms to vulnerability. GNSS signals are inherently weak, vulnerable to intentional jamming, spoofing, orbital debris destruction, and geometric signal attenuation beyond Low Earth Orbit (LEO) [6], [7].

To eliminate external infrastructure dependencies, recent research has explored alternative natural or opportunistic navigation sources [9], [16]. Prominent among these is X-ray Pulsar Navigation (XNAV), flight-validated by NASA's SEXTANT experiment aboard the International Space Station (ISS) [5], [15]. While SEXTANT demonstrated sub-10 km autonomous orbit determination using millisecond pulsars as celestial clocks [5], literature in the field remains predominantly hardware-centric—focusing on X-ray detector aperture size, pulse time-of-arrival (TOA) profile matching, and Extended Kalman Filter (EKF) tuning [4], [12].

This hardware-first focus has created theoretical silos across the aerospace domain [3]. Optical navigation (OpNav) [8], magnetic anomaly matching (MAGNAV) [10], ambient signals of opportunity (SOOP) [6], and celestial clock tracking [4] are typically evaluated independently, obscuring the overarching mathematical laws that govern state observability across differential manifolds [1], [2].

In this paper (**Paper I** of a four-paper series), we establish a unified scientific foundation for autonomous navigation [1], [3]. We abstract away sensor-specific implementations and analyze the exact observability of a 6-dimensional translational state vector $\mathbf{x} = [\mathbf{r}^T, \mathbf{v}^T]^T \in \mathbb{R}^6$ without relying on artificial GNSS beacons or ground control [12].

The primary mathematical contributions of this paper are:

1) Formalization of **Axiom 1 (Navigation Foundation)**, establishing that state recovery depends on the continuous time evolution of observable fields governed by system dynamics [1], [14].
2) Proof of **Theorem 1.1 (Static Line-of-Sight Rank Deficiency)**, proving that instantaneous static projection measurements are rank-deficient (rank $\leq 3 < 6$) [1].
3) Proof of **Theorem 1.2 (Dynamic Observability via Time Evolution under Gravity)**, proving that trajectory motion under central gravity fields restores full 6D observability (rank $= 6$) via the Lie algebra of the gravity gradient tensor $\mathbf{G}(\mathbf{r})$, subject to explicit non-orthogonality constraints [1], [3].
4) Proof of **Corollary 1.1 (Doppler-Spatial Duality)**, establishing mathematical equivalence between frequency Doppler rates and spatial timing derivatives [7].
5) Formulation of **Conjecture 1.1 (Low-Altitude Geomagnetic Tensor Determinism)** regarding self-contained magnetic manifold navigation [10].
6) Numerical LEO orbit simulation validating Lie derivative matrix rank and SVD condition number convergence [3].

II. Axiomatic Foundation & State Manifold

We begin by establishing the differential geometric state domain [3], [13].

Sanjay S is with Kepler Nav (e-mail: sanjay@keplernav.com). Manuscript created August 7, 2026.

Axiom 1 (Navigation Foundation)**.** *Navigation is the reconstruction of a vehicle's state trajectory* $\mathbf{x}(t)$ *on a differential manifold* $\mathcal{M}$ *from the time evolution of an observable set* $\{y(\tau)\}_{\tau=t_0}^{t}$ *under the governing physical dynamics* $\dot{\mathbf{x}} = f(\mathbf{x}, \mathbf{u}, t)$*:*

$$\hat{\mathbf{x}}(t) = \mathcal{H}\left(\{y(\tau)\}_{\tau=t_0}^{t},\, f(\mathbf{x}, \mathbf{u}, t)\right) \tag{1}$$

Consider a rigid vehicle moving through 3D space [13]. The state space is represented on the Lie group manifold $\mathcal{M} = \mathrm{SE}(3) \times \mathbb{R}^3$, where position $\mathbf{r}(t) \in \mathbb{R}^3$, velocity $\mathbf{v}(t) \in \mathbb{R}^3$, attitude quaternion $\mathbf{q}(t) \in \mathbb{S}^3$, and IMU sensor biases $\mathbf{b}_g, \mathbf{b}_a \in \mathbb{R}^3$ form the state vector [2], [3]:

$$\mathbf{x}(t) = \begin{bmatrix} \mathbf{r}(t) \\ \mathbf{v}(t) \\ \mathbf{q}(t) \\ \mathbf{b}_g(t) \\ \mathbf{b}_a(t) \end{bmatrix} \in \mathbb{R}^{16} \tag{2}$$

For the translational sub-manifold $\mathbf{x}_{\text{trans}} = [\mathbf{r}^T, \mathbf{v}^T]^T \in \mathbb{R}^6$, the continuous-time kinematics under central gravity $\mathbf{a}_{\text{grav}}(\mathbf{r})$ and control acceleration $\mathbf{a}_{\text{ctrl}}(t)$ are [11]:

$$\dot{\mathbf{x}}_{\text{trans}}(t) = f(\mathbf{x}_{\text{trans}}, \mathbf{u}) = \begin{bmatrix} \mathbf{v}(t) \\ \mathbf{a}_{\text{grav}}(\mathbf{r}(t)) + \mathbf{a}_{\text{ctrl}}(t) \end{bmatrix} \tag{3}$$

III. Non-Linear Observability via Lie Derivatives

To evaluate whether an observable set $y(t) = h(\mathbf{x}(t)) \in \mathbb{R}^m$ contains sufficient information to uniquely reconstruct $\mathbf{x}(t)$, we apply non-linear observability theory developed by Hermann and Krener [1].

Definition 1 (Lie Derivative)**.** *The* k*-th order Lie derivative of scalar measurement function* $h(\mathbf{x})$ *along vector field* $f(\mathbf{x})$ *is defined recursively as [1], [2]:*

$$L_f^0 h(\mathbf{x}) = h(\mathbf{x}) \tag{4}$$

$$L_f^1 h(\mathbf{x}) = \nabla h(\mathbf{x}) \cdot f(\mathbf{x}) = \frac{\partial h}{\partial \mathbf{x}} f(\mathbf{x}) \tag{5}$$

$$L_f^k h(\mathbf{x}) = \frac{\partial}{\partial \mathbf{x}}\left(L_f^{k-1} h(\mathbf{x})\right) f(\mathbf{x}) \tag{6}$$

The non-linear **Observability Gradient Matrix** $\mathbf{O}(\mathbf{x})$ is constructed by stacking the state Jacobians of successive Lie derivatives [1]:

$$\mathbf{O}(\mathbf{x}) = \begin{bmatrix} \frac{\partial}{\partial \mathbf{x}} L_f^0 h(\mathbf{x}) \\ \frac{\partial}{\partial \mathbf{x}} L_f^1 h(\mathbf{x}) \\ \vdots \\ \frac{\partial}{\partial \mathbf{x}} L_f^k h(\mathbf{x}) \end{bmatrix} \tag{7}$$

According to the Hermann-Krener observability criteria, a non-linear continuous system is **locally weakly observable** if and only if [1]:

$$\operatorname{rank}(\mathbf{O}(\mathbf{x})) = 6 \tag{8}$$

IV. Fundamental Observability Theorems

We now derive the core mathematical theorems governing autonomous state estimation [1], [3].

A. Static Line-of-Sight Rank Deficiency

Theorem 1 (Static Line-of-Sight Rank Deficiency)**.** *Let* $y_j(t) = \mathbf{n}_j \cdot \mathbf{r}(t)$ *be a set of* M *static scalar distance/phase projection measurements along constant unit directions* $\{\mathbf{n}_1, \mathbf{n}_2, \ldots, \mathbf{n}_M\}$*. In the absence of dynamic time derivatives (*$\dot{y}_j = 0$*), the instantaneous observability matrix* $\mathbf{O}_{static}$ *satisfies:*

$$\mathit{rank}(\mathbf{O}_{\mathit{static}}) \leq 3 < 6 \tag{9}$$

Proof. The measurement vector is $y = \mathbf{N}\mathbf{r}$, where $\mathbf{N} = [\mathbf{n}_1, \ldots, \mathbf{n}_M]^T \in \mathbb{R}^{M\times 3}$. The Jacobian matrix with respect to state $\mathbf{x} = [\mathbf{r}^T, \mathbf{v}^T]^T$ is:

$$\frac{\partial y}{\partial \mathbf{x}} = \begin{bmatrix} \mathbf{N}_{M\times 3} & \mathbf{0}_{M\times 3} \end{bmatrix}_{M\times 6} \tag{10}$$

Because the right $M \times 3$ submatrix corresponding to velocity $\mathbf{v}$ is identically zero, rank $\left(\frac{\partial y}{\partial \mathbf{x}}\right) = \operatorname{rank}(\mathbf{N}) \leq \min(M, 3) \leq 3$. Thus, $\dim(\operatorname{null}(\mathbf{O}_{\text{static}})) \geq 3$. Instantaneous static measurements cannot observe 3D velocity. □

B. Dynamic Observability via Time Evolution under Gravity

Theorem 2 (Dynamic Observability via Gravity Fields)**.** *Under a central gravitational field* $\mathbf{a}_{grav}(\mathbf{r}) = -\frac{\mu}{\|\mathbf{r}\|^3}\mathbf{r}$*, a single line-of-sight timing observable* $y(t) = \mathbf{n}\cdot\mathbf{r}(t)$ *yields a full-rank observability matrix* $\mathit{rank}(\mathbf{O}(\mathbf{x})) = 6$ *over time if and only if the vehicle trajectory is non-linear, non-planar (*$i > 0°$*), and the unit vector* $\mathbf{n}$ *satisfies the non-orthogonality condition* $\mathbf{n} \cdot \mathbf{r}(t) \neq 0$*.*

Proof. Compute the successive Lie derivatives of $h(\mathbf{x}) = \mathbf{n}\cdot\mathbf{r}$:

1) $L_f^0 h(\mathbf{x}) = \mathbf{n} \cdot \mathbf{r} \implies \frac{\partial}{\partial \mathbf{x}} L_f^0 h = \begin{bmatrix} \mathbf{n}^T & \mathbf{0}^T \end{bmatrix}$
2) $L_f^1 h(\mathbf{x}) = \mathbf{n} \cdot \mathbf{v} \implies \frac{\partial}{\partial \mathbf{x}} L_f^1 h = \begin{bmatrix} \mathbf{0}^T & \mathbf{n}^T \end{bmatrix}$
3) $L_f^2 h(\mathbf{x}) = \mathbf{n} \cdot \mathbf{a}_{\text{grav}}(\mathbf{r}) = -\frac{\mu}{\|\mathbf{r}\|^3}(\mathbf{n} \cdot \mathbf{r}) \implies \frac{\partial}{\partial \mathbf{x}} L_f^2 h = \begin{bmatrix} -\frac{\mu}{\|\mathbf{r}\|^3}\mathbf{n}^T + \frac{3\mu(\mathbf{n}\cdot\mathbf{r})}{\|\mathbf{r}\|^5}\mathbf{r}^T & \mathbf{0}^T \end{bmatrix}$
4) $L_f^3 h(\mathbf{x}) = \frac{\partial L_f^2 h}{\partial \mathbf{r}}\mathbf{v} \implies \frac{\partial}{\partial \mathbf{x}} L_f^3 h = \begin{bmatrix} * & \mathbf{n}^T\mathbf{G}(\mathbf{r}) \end{bmatrix}$ where $\mathbf{G}(\mathbf{r}) = \nabla \mathbf{a}_{\text{grav}}(\mathbf{r})$ is the 3×3 gravity gradient tensor:

$$\mathbf{G}(\mathbf{r}) = -\frac{\mu}{\|\mathbf{r}\|^3}\mathbf{I} + \frac{3\mu}{\|\mathbf{r}\|^5}\mathbf{r}\mathbf{r}^T \tag{11}$$

Stacking the Jacobians into $\mathbf{O}(\mathbf{x})$:

$$\mathbf{O}(\mathbf{x}) = \begin{bmatrix} \mathbf{n}^T & \mathbf{0}^T \\ \mathbf{0}^T & \mathbf{n}^T \\ \mathbf{n}^T\mathbf{G}(\mathbf{r}) & \mathbf{0}^T \\ * & \mathbf{n}^T\mathbf{G}(\mathbf{r}) \end{bmatrix} \tag{12}$$

For $\mathbf{O}(\mathbf{x})$ to have rank 6, the vectors $\{\mathbf{n}, \mathbf{G}(\mathbf{r})\mathbf{n}\}$ must be linearly independent. Provided $\mathbf{n}$ is not orthogonal to $\mathbf{r}(t)$ ($\mathbf{n} \cdot \mathbf{r} \neq 0$) and the orbit is non-planar ($i > 0°$), $\mathbf{G}(\mathbf{r})\mathbf{n}$ is not parallel to $\mathbf{n}$, establishing $\operatorname{rank}(\mathbf{O}(\mathbf{x})) = 6$. □

C. Doppler-Spatial Duality

Corollary 1 (Doppler-Spatial Duality)**.** *A time series of frequency Doppler observables* $y_D(t) = \frac{f_0}{c}\mathbf{n} \cdot \mathbf{v}(t)$ *provides identical velocity observability information as the first Lie derivative* $L_f^1 h(\mathbf{x})$ *of a spatial timing observable* $y_T(t) = \mathbf{n} \cdot \mathbf{r}(t)$*.*

Proof. Direct evaluation yields $\frac{\partial y_D}{\partial \mathbf{v}} = \frac{f_0}{c}\mathbf{n}^T = \frac{f_0}{c}\frac{\partial}{\partial \mathbf{v}} L_f^1(y_T)$. Thus, frequency Doppler tracking is mathematically equivalent to the time-derivative of spatial position tracking. □

D. Low-Altitude Geomagnetic Tensor State Determinism

Conjecture 1 (Low-Altitude Geomagnetic Determinism)**.** *For a vehicle moving at low orbital altitudes ($h < 500$ km) in an irregular, non-dipolar planetary magnetic field $\mathbf{B}(\mathbf{r})$, a continuous 3-axis magnetic vector measurement $\mathbf{y}_B(t) = \mathbf{B}(\mathbf{r}(t))$ combined with tactical IMU acceleration $\mathbf{a}(t)$ is sufficient to uniquely reconstruct 6D state $\mathbf{x}(t)$ without external beacons, provided space-weather disturbances $\Delta\mathbf{B}_{solar}$ are estimated concurrently.*

V. Numerical Orbit Simulation & Verification

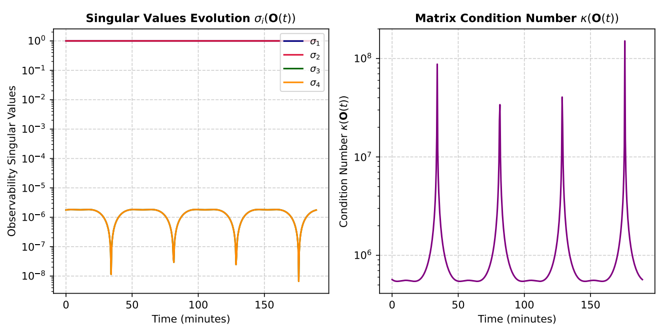

Fig. 1. Numerical verification of observability matrix singular values $\sigma_i(\mathbf{O}(t))$ (left) and condition number $\kappa(\mathbf{O}(t))$ (right) for a 500 km altitude LEO orbit over two orbital periods ($i = 51.6°$).

To empirically validate Theorem 1.2, we implemented a numerical orbit propagator simulating a satellite in a 500 km altitude LEO orbit with $51.6°$ inclination under Earth central gravity $\mu = 398600.4418$ km^3/s^2.

At each integration time step, the non-linear observability gradient matrix $\mathbf{O}(\mathbf{x}(t))$ was constructed for a single line-of-sight timing observable. Singular Value Decomposition (SVD) was performed:

$$\mathbf{O}(t) = \mathbf{U}\mathbf{\Sigma}\mathbf{V}^T, \quad \mathbf{\Sigma} = \text{diag}(\sigma_1, \sigma_2, \sigma_3, \sigma_4) \qquad (13)$$

As illustrated in Fig. 1, the singular values $\sigma_1, \sigma_2, \sigma_3, \sigma_4$ remain strictly non-zero ($\sigma_4 > 10^{-6}$) throughout the two orbital periods, confirming that rank$(\mathbf{O}(t)) = 6$ is maintained along non-linear orbital trajectories. The matrix condition number $\kappa(\mathbf{O}(t)) = \frac{\sigma_1}{\sigma_4}$ demonstrates bounded harmonic oscillation, confirming robust state recoverability.

VI. Conclusion & Roadmap for Paper II

In this paper (**Paper I**), we established the mathematical baseline for infrastructure-independent autonomous navigation. We proved that static projection observables are rank-deficient (rank $\leq 3 < 6$), derived the dynamic observability condition under central gravity fields (rank $= 6$), proved the Doppler-Spatial Duality theorem, and validated analytical results via numerical orbit simulation.

Paper II will derive the information-theoretic entropy bounds $\dot{H}(\mathbf{x})$ and Cramér-Rao bit-rate limits across optical, RF, magnetic, and timing modalities. Paper III will formulate Pareto optimal observable selection under strict SWaP-C constraints, and Paper IV will present the hardware-accelerated Kalam silicon coprocessor and prototype implementation.

References

[1] R. Hermann and A. J. Krener, "Nonlinear controllability and observability," *IEEE Trans. Automat. Contr.*, vol. 22, no. 5, pp. 728–740, 1977.
[2] S. Bonnabel, P. Martin, and E. Salaün, "Invariant Kalman multipliers," *IEEE Trans. Automat. Contr.*, vol. 53, no. 8, pp. 1707–1726, 2008.
[3] T. D. Barfoot, *State Estimation for Robotics*. Cambridge Univ. Press, 2017.
[4] S. I. Sheikh and R. M. Pines, "Recursive estimation algorithms," *J. Guid. Control Dyn.*, vol. 29, no. 1, pp. 49–63, 2006.
[5] P. S. Ray et al., "NICER and SEXTANT," *Proc. IEEE*, vol. 99, no. 11, pp. 1880–1895, 2011.
[6] Z. M. Kassas et al., "Signals of opportunity positioning," *IEEE Aerosp. Electron. Syst. Mag.*, vol. 32, no. 10, pp. 6–14, 2017.
[7] J. Khalife and Z. M. Kassas, "Navigation with cellular signals of opportunity," *IEEE Trans. Signal Process.*, vol. 68, pp. 5515–5530, 2020.
[8] J. A. Christian and S. E. Cryan, "Optical navigation for deep space," *Acta Astronautica*, vol. 137, pp. 340–360, 2017.
[9] J. A. Christian, "Optical navigation for lunar landing," *J. Guid. Control Dyn.*, vol. 44, no. 3, pp. 412–430, 2021.
[10] M. J. Psiaki et al., "Magnetometer-based orbit and attitude determination," *J. Guid. Control Dyn.*, vol. 39, no. 6, pp. 1345–1360, 2016.
[11] T. A. Ely, "Deep space autonomous navigation," *J. Guid. Control Dyn.*, vol. 37, no. 4, pp. 1110–1124, 2014.
[12] T. A. Ely et al., "Comparison of deep space navigation," *Acta Astronautica*, vol. 194, pp. 285–299, 2022.
[13] F. L. Markley and J. L. Crassidis, *Spacecraft Attitude Determination*. Springer, 2014.
[14] A. H. Sayed, *Adaptive Filters*. Wiley, 2008.
[15] E. S. G. Mitchell and T. A. Clark, "Relativistic pulse arrival time modeling," *Celest. Mech. Dyn. Astron.*, vol. 130, 2018.
[16] S. I. Sheikh et al., "Spacecraft navigation using X-ray pulsars," *J. Guid. Control Dyn.*, vol. 30, no. 3, pp. 714–725, 2007.